Global-scale abrupt climate events and black swans: an ice-core-derived palaeoclimate perspective from Earth's highest mountains

LONNIE G. THOMPSON[1,2]*, ELLEN MOSLEY-THOMPSON[1,3], MARY E. DAVIS[1], STACY E. PORTER[1], DONALD V. KENNY[1] & PING-NAN LIN[1]

[1]*Byrd Polar and Climate Research Center, The Ohio State University, Columbus OH 43210, USA*

[2]*School of Earth Sciences, The Ohio State University, Columbus OH 43210, USA*

[3]*Department of Geography, The Ohio State University, Columbus OH 43210, USA*

**Correspondence: thompson.3@osu.edu*

Abstract: High-elevation tropical glaciers provide records of past climate from which current changes can be assessed. Comparisons among three ice-core records from tropical mountains on opposite sides of the Pacific Ocean reveal how climatic events are linked through large-scale processes such as El Niño–Southern Oscillation. Two distinctive trans-Pacific events in the mid-fourteenth and late-eighteenth centuries are distinguished by elevated aerosol concentrations in cores from the Peruvian Andes and the Tibetan Himalaya. Today aerosol sources for these areas are enhanced by droughts accompanying El Niños. In both locations, large-scale atmospheric circulation supports aerosol transport from likely source regions. Oxygen isotopic ratios from the ice cores are significantly linked with tropical Pacific sea-surface temperatures, especially in the NIÑO3.4 region. The arid periods in the fourteenth and eighteenth centuries reflect droughts that were possibly connected to strong and/or persistent El Niño conditions and Intertropical Convergence Zone migration. These 'black swans' are contemporaneous with climate-related population disruptions. Recent warming, particularly at high elevations, is posing a threat to tropical glaciers, many of which have been retreating at unprecedented rates over the last several thousand years. The diminishing ice in these alpine regions endangers water resources for populations in South Asia and South America.

Tropical ice fields are sensitive indicators and recorders of climate changes, and cores drilled from the glaciers, ice caps and ice sheets throughout the world offer unique records of climatic and environmental change over a wide range of temporal and spatial scales. Ice preserves records of regional- to global-scale temperature, precipitation, atmospheric circulation and atmospheric chemistry. With some exceptions, ice-core records from outside the polar regions are of relatively short duration (<12 ka); however, they are of very high (seasonal to decadal) resolution and are therefore capable of preserving evidence of abrupt climatic events which are of vital importance to human populations. In order to capture the complex variability that occurs in the tropical climate system, a global array of low-latitude ice-core records is required (Fig. 1). When viewed in tandem, these climate records illustrate both regional differences on decadal to centennial timescales and hemispheric and global similarities on millennial timescales. For example, changes in ice-core $\delta^{18}O$ from the end of the last glacial stage to the Early Holocene, where recorded, are of comparable magnitude (*c.* 4–6‰) (Thompson *et al.* 2005).

A select few ice cores provide records at annual resolution over hundreds of years that reveal magnitudes and rates of abrupt climate change (Thompson *et al.* 2000, 2013). When large, infrequent climate events of interhemispheric extent occur it is highly likely that these ice fields record them. In the low latitudes, alpine ice fields exist in fairly stable but sensitive environments where mid-tropospheric temperatures vary within a relatively narrow range. Since the early 1980s, much effort has been expended to retrieve ice cores from relatively small high-altitude ice caps in the tropics, primarily from regions that are very sensitive to tropical Pacific influences such as the central Andes and the Tibetan Plateau/Himalaya ('Third Pole') region.

The tropics (30° N to 30° S), which cover 50% of Earth's total surface area, are known as Earth's 'heat engine'. Approximately 37% of the world's oceans lie between 20° N and 20° S. Tropical evaporation, driven by warm sea-surface temperatures (SSTs), dominates the water vapour flux into the global atmosphere (Fig. 1a, b). This vapour flux is one of the primary controls on stable isotopes ($\delta^{18}O$, δD) in precipitation. On interannual timescales, climate

From: Pant, N. C., Ravindra, R., Srivastava, D. & Thompson, L. G. (eds) 2018. *The Himalayan Cryosphere: Past and Present*. Geological Society, London, Special Publications, **462**, 7–22.
First published online September 29, 2017, https://doi.org/10.1144/SP462.6

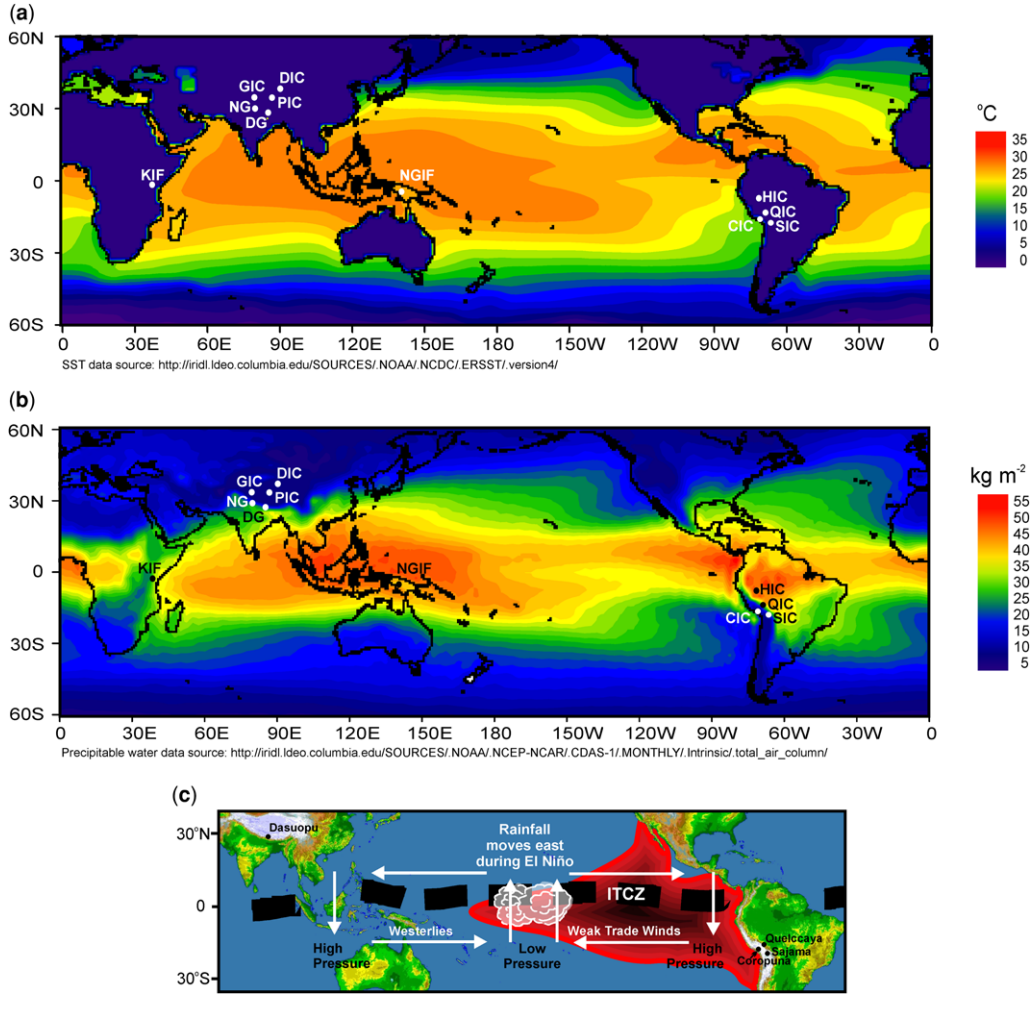

Fig. 1. (**a**) Reconstructed sea-surface temperatures (annual averages from 1997 to 2015) (Rayner *et al.* 2003) in tropical and middle latitudes are approximately coincident with (**b**) reanalysis data of atmospheric precipitable water concentrations (Kalnay *et al.* 1996); highest values of both occur between 30° N and 30° S. Ohio State University ice-core sites are marked in both (a) and (b) as: KIF, Kilimanjaro ice field; NG, Naimona'nyi glacier; GIC, Guliya ice cap; DG, Dasuopu glacier (where the DSC was drilled); PIC, Puruogangri ice cap; DIC, Dunde ice cap; NGIF, New Guinea ice fields; CIC, Coropuna ice cap (where the CCC was drilled); HIC, Huascarán ice cap; QIC, Quelccaya ice cap (where the QSC was drilled); and SIC, Sajama ice cap (where the SSC was drilled). (**c**) Map of tropical Pacific Basin region showing ENSO components along with the Intertropical Convergence Zone (ITCZ, heavy dashed line). Black filled circles depict the Dasuopu Glacier in the central Himalaya and Quelccaya, Coropuna and Sajama on the Peruvian/Bolivian Altiplano.

over the tropical Pacific Ocean is dominated by the interconnected oceanic–atmospheric phenomenon known as the El Niño–Southern Oscillation (ENSO), which involves the interaction between central and eastern equatorial Pacific SSTs and upper and lower atmospheric circulation driven by pressure dipoles (Fig. 1c). The equatorial ocean warming produced by ENSO is responsible for meteorological phenomena that directly or indirectly affect much of Earth's tropical and extratropical regions and their populations. In fact, ENSO and the Indian Summer Monsoon (ISM) are intricately linked (Walker & Bliss 1932). Continental precipitation patterns associated with specific El Niño events and monsoon failures are not uniformly consistent; however, strong events are often marked by increased aridity throughout much of the tropics. Major drought events, both ENSO and non-ENSO

related, are recorded in ice cores recovered from these regions (Thompson *et al.* 1992, 2000, 2013).

Here we examine the teleconnections across the tropical Pacific Ocean between the Peruvian/Bolivian Andes and the Himalaya. In particular, two distinct events in the mid-fourteenth century and in the late-eighteenth century, are distinguished by very high concentrations of aerosols contemporaneously preserved in ice cores from these widely separated regions. We explore the linkages between ice-core chemistry and ENSO conditions and the role that enhanced ENSO may have played. A discussion is presented on the categorization of these events as 'black swans', which are unpredictable phenomena with major repercussions that are explainable only after the fact.

The records

All ice cores drilled from the tropical glaciers and ice caps discussed here have been analysed for stable isotopes of oxygen ($\delta^{18}O$) and concentrations of mineral dust and major ions (fluoride F^-, chloride Cl^-, sulphate SO_4^{2-}, nitrate NO_3^-, sodium Na^+, ammonium NH_4^+, potassium K^+, magnesium Mg^{2+} and calcium Ca^{2+}). The temporal resolution of the records depends upon the annual rate of snow accumulation (annual net balance, or A_n). The high A_n of many of these glaciers allows annual dating using seasonal variations in two or more of these parameters over at least the last *c.* 250 years. Cores recovered from more arid regions where A_n is low and/or current ablation and melting are extreme (e.g. Guliya on the Tibetan Plateau, Kilimanjaro) are not resolvable, or at least not easily resolvable, at annual resolution. Instead, their time series are reconstructed using alternate methods (Thompson *et al.* 1997, 2002).

Here we emphasize ice-core-derived climate records from three high-accumulation sites: (1) the Coropuna crater core (CCC) from the summit of the Coropuna ice cap (CIC), location 15° 32′ S, 72° 39′ W, 6450 m above sea level (m asl); (2) the Quelccaya summit core (QSC) from the Quelccaya ice cap (QIC), location 13° 56′ S, 70° 50′ W, 5670 m asl in southern Peru; and (3) the Dasuopu summit core (DSC) from the Dasuopu glacier (DG), location 28° 23′ N, 85° 43′ E, 7200 m asl in the central Himalaya, Tibet (Fig. 1). The CCC record is annually resolved to the mid-eighteenth century, the DSC record to the mid-fifteenth century and the QSC record yields a climate history at annual resolution over 18 centuries. Constructions of the DSC and QSC timescales are discussed in previous publications (Thompson *et al.* 2000, 2013), while construction of the CCC timescale is demonstrated in Figure 2.

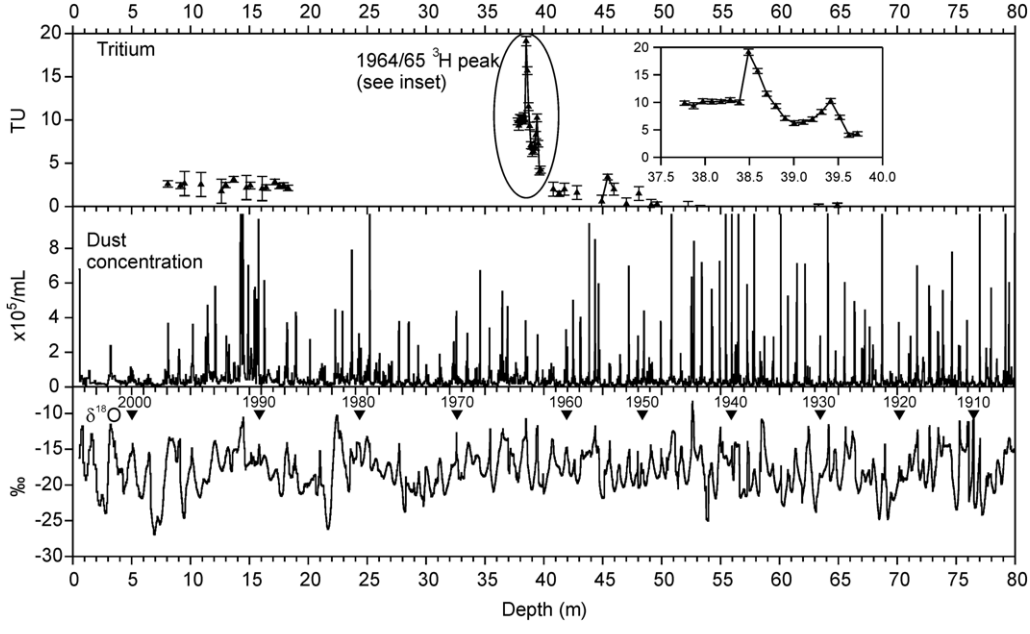

Fig. 2. Timescale development of ice-core records is demonstrated in the top 80 m of the Coropuna ice core (CCC) showing selection of years back to 1910 CE using summer (wet) and winter (dry) seasonal oscillations in dust concentration and $\delta^{18}O$. The twentieth-century timescale is calibrated with the 1964/65 ^3H peak (residue from thermonuclear testing) at 38.5 m.

Each of these three cores, along with the Sajama summit core (SSC) from the ice cap on Nevado Sajama (SIC), location 18° 06′ S, 68° 52′ W, 6542 m asl on the Bolivian Altiplano (Thompson *et al.* 1998), contains a prominent event in the late eighteenth century characterized by highly elevated concentrations of F^- and Cl^- (Fig. 3a–d). Peaks in other ion concentrations and mineral dust occur at this time in the DSC, CCC and SSC; however, they are not observed in the QSC (Table 1). Although the high F^- and Cl^- concentrations in the QSC are difficult to explain in the absence of the cations necessary to form salts, they do not appear to be of volcanic origin since no large eruptions are evident at this time in

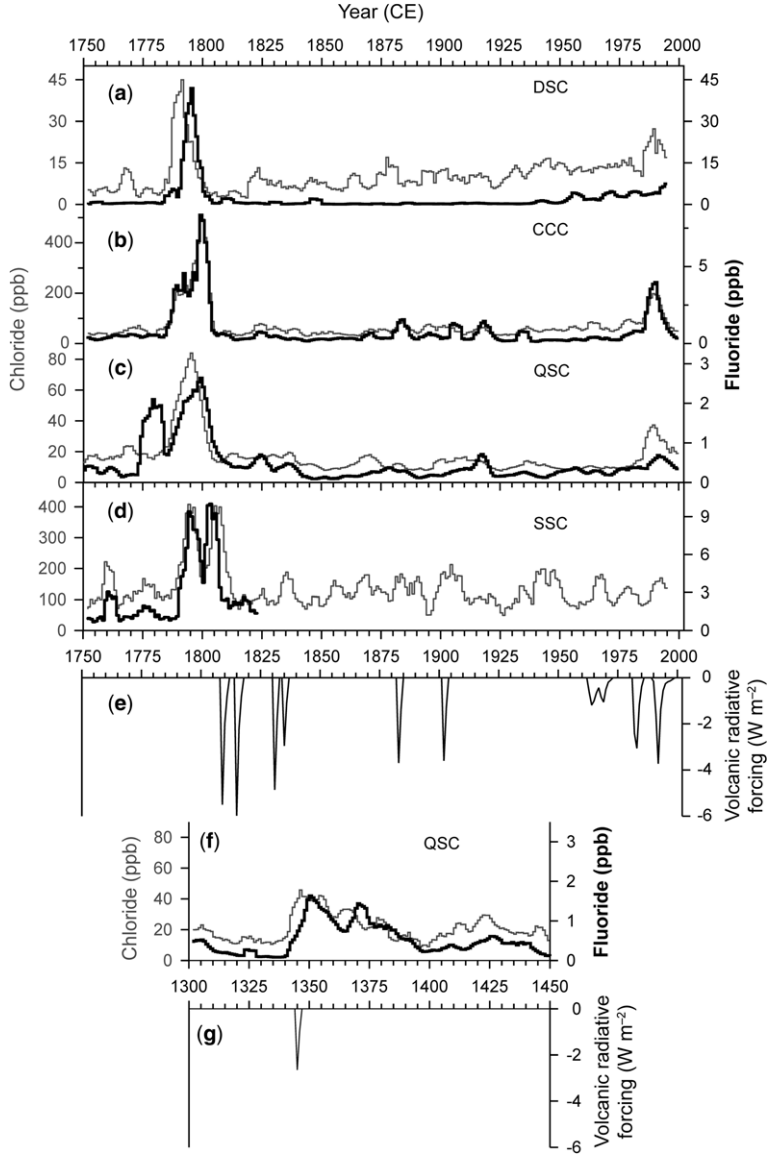

Fig. 3. Five-year running means of Cl^- (light line) and F^- (heavy line) from 1750 to 2002 CE for: (**a**) the DSC; (**b**) the CCC; (**c**) the QSC; and (**d**) the SSC. F^- data for the SSC exist only from 1750 to 1825 CE. (**e**) Volcanic climate forcing of the tropical Pacific (Mann *et al.* 2005) is shown for the same period. (**f**) Time series of 5-year running means of Cl^- (light line) and F^- (heavy line) in the QSC are shown with (**g**) volcanic forcing (Mann *et al.* 2005) from 1300 to 1450 CE.

Table 1. *Averages of major ion (ppb) and mineral dust ($\times 10^5$/mL) concentrations and $\delta^{18}O$ in four tropical ice cores for the late-eighteenth-century event and the ±25 year background before and after the event*

		F^-	Cl^-	SO_4^{2-}	NO_3^-	Na^+	NH_4^+	K^+	Mg^{2+}	Ca^{2+}	Dust per mL	$\delta^{18}O$ per mil
Quelccaya summit core (QSC) Annual snow accumulation = *c.* 1000 mm												
1786–1802	Event	2.1	60.3	0.7	44.3	2.5	57.7	0.9	0.1	0.4	23 782	−18.60
	Background	0.5	16.4	10.9	118.6	11.2	67.7	1.1	0.2	2.4	27 669	−18.94
	BG SD*	0.6	3.6	38.0	86.8	33.1	27.1	2.0	0.5	7.8	8594	1.7
	% difference	**320**	**265**	−94	−63	−78	−15	−18	−50	−83	−14	2
Coropuna caldera core (CCC) Annual snow accumulation = *c.* 700 mm												
1788–1803	Event	7.0	300.9	705.6	247.5	82.5	141.4	32.9	17.0	154.3	161 898	−16.45
	Background	0.6	49.4	193.6	170.7	27.8	72.5	8.1	7.3	48.8	148 648	−19.39
	BG SD*	0.5	27.2	97.5	64.7	17.8	23.8	4.7	4.4	46.4	135 725	2.4
	% difference	**1067**	**509**	**264**	45	**197**	95	**306**	**133**	**216**	9	15
Sajama summit core (SSC)† Annual snow accumulation = *c.* 440 mm												
1790–1806	Event	7.1	281.3	1045.7	255.1	111.1	284.0	995.8	252.9	111.1	277 066	−15.86
	Background	1.6	138.9	565.1	210.0	82.2	137.8	582.4	220.4	82.2	178 630	−18.40
	BG SD*	1.2	109.3	394.3	72.3	65.8	105.5	318.9	78.4	65.8	138 999	2.4
	% difference	**344**	**103**	85	21	35	**106**	71	15	35	55	14
Dasuopu summit core (DSC) Annual snow accumulation = *c.* 1000 mm												
1787–1799	Event	20.1	27.6	56.8	81.8	37.8	44.7	11.3	8.0	227.2	90 134	−19.15
	Background	0.9	5.7	18.6	45.50	13.9	32.8	7.8	3.0	77.1	31 790	−20.71
	BG SD*	0.6	3.6	38.0	86.8	33.1	27.1	2.0	0.5	7.8	8594	1.7
	% difference	**2133**	**384**	**205**	80	**172**	36	45	**167**	**195**	**184**	8

Percentage difference between the event and background greater than 100% are in bold font.
*Standard deviations for the backgrounds (BG SD) and percentage differences between each parameter during and around the event are also shown.
†Cation and F^- data are available only between 1750 and 1825 CE; the background therefore covers 25 years prior to the beginning of the event and 19 years after the end of the event.

the record of tropical Pacific volcanic radiative forcing (Mann *et al.* 2005) (Fig. 3e).

An earlier event marked by elevated F^- and Cl^- concentrations begins at *c.* 1340 CE in the well-dated QSC and tapers off at *c.* 1395 CE (Fig. 3f). Although the concentrations are *c.* 50% lower than in the late eighteenth century peak they are sustained over multiple decades and, like the later event, are not accompanied by increases in other major ions and are not concurrent with major tropical volcanic eruptions (Fig. 3g). In the DSC, where propagating dating errors allow decadal resolution at best below 1440 CE, the fourteenth-century event is expressed more subtly by small increases in Cl^- and mineral dust concentrations. Lack of solid time control below 1750 CE in the CCC and the SSC prevents definitive identification of the earlier event in those records.

Geological and meteorological settings

Glaciers in both the central Himalaya and the central Andes are located in high mountain ranges in close proximity to and downwind of dry, saline areas containing halogen-rich groundwater (Fig. 4). To the south and west of the Himalaya, the groundwater has unusually high concentrations of F^- (>1.5 ppm) from clay-rich soils (Rao & Devadas 2003; Edmunds & Smedley 2013) derived from granitic rocks containing F^--bearing minerals (Fig. 4a). Sodic soils and groundwater with elevated F^- are present in the hard rock areas south of the Ganges Valley and in the arid northwestern part of India (Jacks *et al.* 2005). Concentrations that are enhanced by increased evapotranspiration and elevated levels of soil-derived F^- have been detected in monsoon rains (Satsangi *et al.* 1998). Near-surface wind vectors during 12 monsoon seasons in June to August (JJA) since 1950, which are distinguished by high F^- and Cl^- concentrations in the DSC, demonstrate direct transport of aerosols to Dasuopu. Potential source areas (PSAs) for ions in the DSC can also be inferred by comparing molar ratios of Na^+/Cl^- in the ice core with those in groundwater and rainwater in northern and western India, respectively, as well as in the water in the major river systems in the Himalaya (Dalai *et al.* 2002; Hren *et al.* 2007) (Table 2). The ratio in the 1790s event in the DSC is comparable to that in PSAs in rainwater in Andhra Pradesh (Rao & Devadas 2003) and groundwater in Western Uttar Pradesh (Saxena *et al.* 1996), both of which are upwind of the DG (Table 2, Fig. 4a). Chemical weathering of evaporites in Himalayan river drainage basins are also an important source of calcium (Dalai *et al.* 2002; Hren *et al.* 2007), which occurs at higher concentrations than the other major ions in the DSC (Table 1).

Across the Pacific Basin, the Peruvian/Bolivian Altiplano is an elevated, arid region with large lakes (e.g. Lake Titicaca (LT)) and desiccated salt flats including the largest, Salar de Uyuni (Rettig

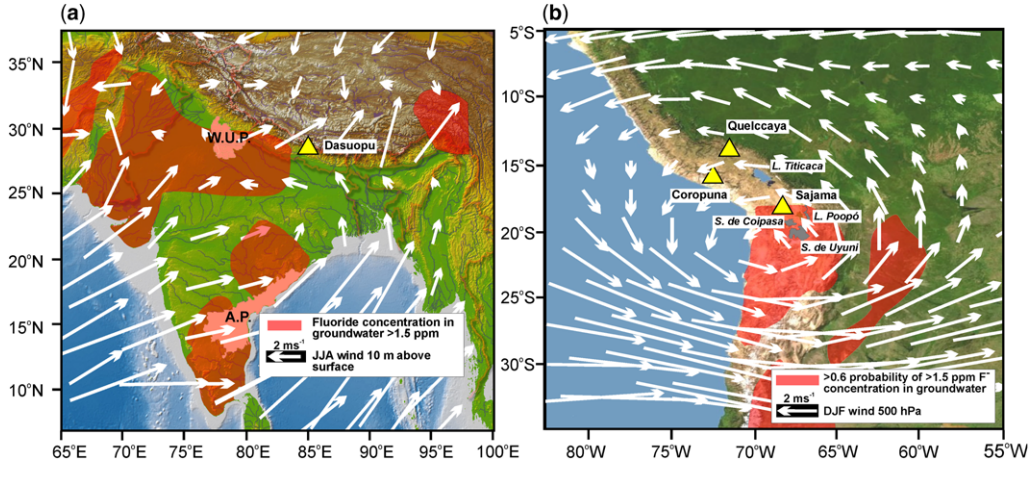

Fig. 4. (**a**) Map of India and the Himalaya with areas of groundwater high in Fl^- concentrations (red shading) (Edmunds & Smedley 2013) and summer monsoon (JJA) near-surface (10 m) wind vectors (NOAA NCEP CDAS 1) for years in the DSC with high Fl^- and Cl^- concentrations (1951, 1952, 1956, 1957, 1958, 1961, 1971, 1978, 1982, 1988, 1992, 1994). Many correspond to El Niño events. Western Uttar Pradesh (W.U.P.) and Andhra Pradesh (A.P.) are outlined. (**b**) Map of the Peruvian/Bolivian Altiplano with areas of >0.6 probability for high (>1.5 ppm) groundwater Fl^- concentrations (Amini *et al.* 2008) (red shading) and austral summer (DJF) 500 hPa wind vectors (NOAA NCEP CDAS 1) for 13 years in the QSC and CCC with high Fl^- and Cl^- concentrations (1965/66, 1982/83, 1986/87, 1987/88, 1988/89, 1989/90, 1990/91, 1992/93, 1993/94, 1994/95, 1995/96, 1996/97 and 2000/01).

Table 2. *Molar ratios of Na^+/Cl^- in the 1790s dust event and the background in each of the ice cores and from potential source areas*

Site		Average Na^+/Cl^- (molar ratio)
Dasuopu glacier	Event	2.12
	Background	3.74
Andhra Pradesh, India*	Pre-monsoon groundwater	1.92
	Post-monsoon groundwater	2.05
Western Uttar Pradesh, India†	Rainwater	2.31
Yamuna river system‡	River water	3.60
Quelccaya ice cap	Event	0.06
	Background	1.04
Coropuna ice cap	Event	0.42
	Background	0.87
Sajama ice cap	Event	0.61
	Background	0.91
Bolivian Altiplano§	Inflow to L. Titicaca	1.05
	Outflow from L. Titicaca	1.06
	Inflow to L. Poopó	1.07
	SW of L. Poopó	1.07
	Salar de Coipasa	0.85

*Rao & Devadas (2003); †Saxena *et al.* (1996); ‡Dalai *et al.* (2002); §Rettig *et al.* (1980)

et al. 1980) (Fig. 4b). Drought preconditions the surface material for atmospheric entrainment. In the austral summer from December to February (DJF) 500 hPa winds circulating anticlockwise pass directly over the salars and the LT region before reaching these Altiplano glaciers. Of the three Altiplano sites, Sajama is located closest to the salars while Quelccaya is furthest. Background concentrations of major ions in the ice cores, along with molar ratios of Na^+/Cl^- (SSC > CCC > QSC) (Tables 1 & 2) suggest a simple back-trajectory pointing to the salars in this highly arid region as the primary PSA. The molar ratio of Na^+/Cl^- in the SSC during the late eighteenth century event is the closest to that of the Salar de Coipasa (0.85) (Rettig *et al.* 1980), while the background ratios in all four cores are comparable to the salar ratio and the outflow and inflow from Lakes Titicaca and Poopó (Fig. 4b). Elevation differences (SIC > CIC > QIC) and annual snow accumulation rates (QIC > CIC > SIC) may also have some effect on the relative ionic concentrations.

Glaciers such as Quelccaya are an important water source for LT during dry austral winters. Over 90% of the lake's water loss is due to evaporation (Roche *et al.* 1992), and El Niño events are marked by increased aridity in this region. LT discharges into the salars to the south (Fig. 4b) so lake level decreases would eventually result in desiccation of these highly saline features. Jacks *et al.* (2005) determined that in India repeated water logging and subsequent evapotranspiration accelerate the development of salinity and sodicity; this may also be the case on the Altiplano.

Concentrations of F^- and Cl^- in the CCC and, to a lesser extent in the QSC, rose in the late 1980s and peaked in the early 1990s (Fig. 3b, c). Extremely arid conditions resulted from the 1987 El Niño and the more persistent El Niños between 1990 and 1995 (Trenberth & Hoar 1997). From 1990 to 1995 however, Volcán Sabancaya, 90 km SE of Coropuna, erupted frequently and may have emitted gaseous F^- and Cl^- into the atmosphere. Moreover, the tropical volcanic radiative forcing (Fig. 3e) reveals a large influx of eruption products to the atmosphere in the 1990s, likely from Mt Pinatubo in the Philippines. Distinguishing the possible sources of F^- and Cl^-, whether volcanic or climatic in origin, to the glaciers in this recent period is not possible. However, no other known tropical volcanic eruptions occurred between 1750 and 2002 CE and between 1300 and 1450 CE that are contemporaneous with Cl^- or F^- peaks in these Andean ice core records. In addition, since the late eighteenth century some contemporaneous F^- events are recorded in the Dasuopu glacier (Fig. 3a), which is 22 000 km away (Fig. 1).

ENSO/monsoon connections

Atmospheric and surface oceanic processes in the tropical Pacific link the climate over the Altiplano with that of the southern Himalaya, and this has been demonstrated by the relationship between $\delta^{18}O$ in tropical ice cores and equatorial Pacific SSTs (Bradley *et al.* 2003; Thompson *et al.* 2011, 2013). Figure 5a–c illustrates the strong similarities

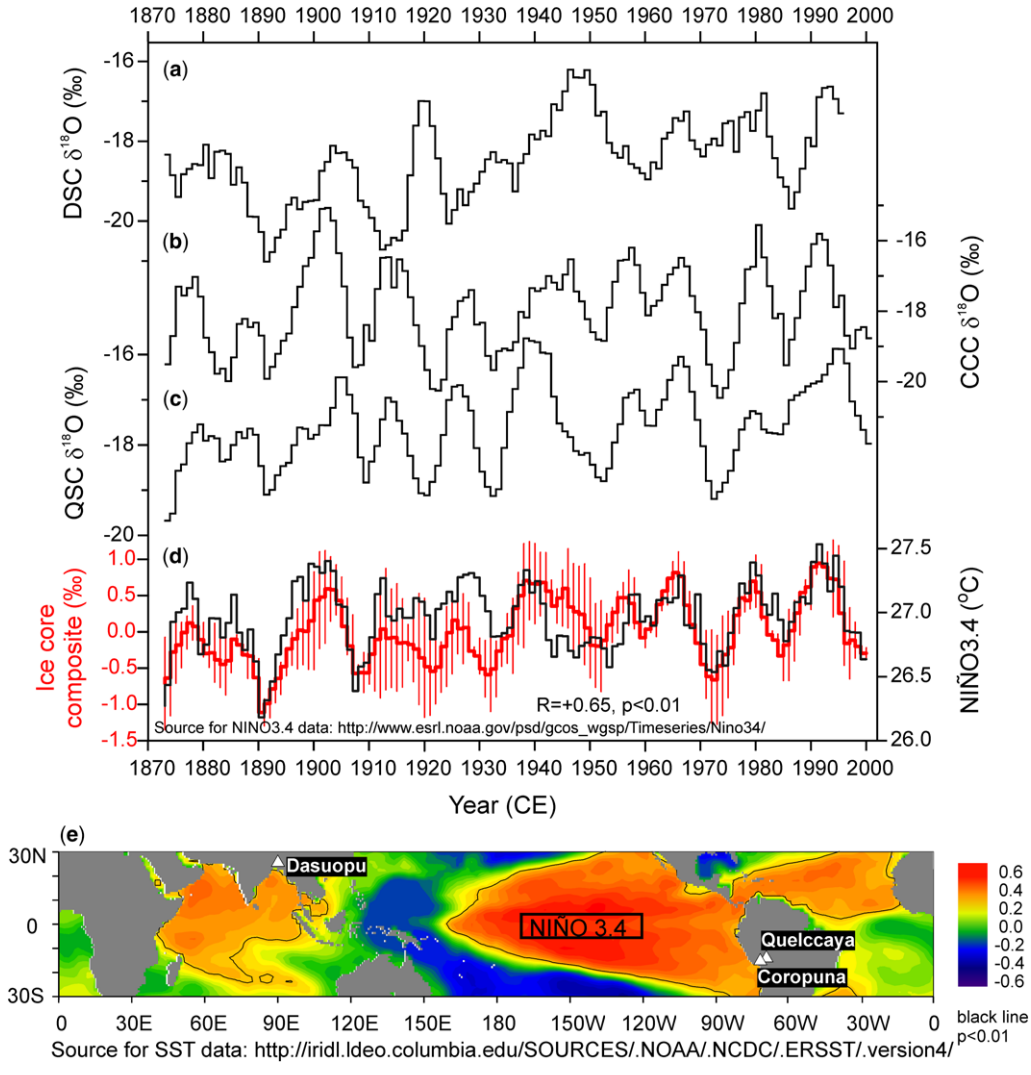

Fig. 5. Comparisons between 5-year running means of $\delta^{18}O$ from: (**a**) the DSC from the Northern Hemisphere and (**b**) the CCC and (**c**) the QSC from the Southern Hemisphere. (**d**) A composite of the three ice-core records shows a significant correlation with the 5-year running means of the NIÑO3.4 index region (Rayner *et al.* 2003) calculated as thermal years (TY), that is, July to June. Standard deviations of the composite record are shown as red vertical bars. (**e**) A spatial correlation between SSTs (Huang *et al.* 2015; Liu *et al.* 2015) and the ice-core composite from 1870 to 2002 CE (no time series smoothing) shows high levels of significance ($p < 0.01$, black lines) in the northern Indian Ocean, the northern tropical Atlantic Ocean and the central and eastern Pacific Ocean.

between the DSC, CCC and QSC $\delta^{18}O$ records, all smoothed with 5-year moving averages. A composite $\delta^{18}O$ time series of the three cores from 1870 to 2002 CE, calculated by averaging the z-scores of the three records, is significantly correlated ($R = +0.65$, $p < 0.01$) with SSTs in the NIÑO3.4 region of the central equatorial Pacific Ocean (5° N to 5° S, 120–170° W; Fig. 5d). This suggests a strong relationship between the coupled tropical ocean/atmosphere system and the stable isotope chemistry of tropical precipitation. Viewing these relationships spatially illustrates highly significant correlations, even without time series smoothing, between the ice-core $\delta^{18}O$ composite and SSTs in large areas of the western tropical Atlantic, the Indian Ocean and the eastern tropical Pacific (Fig. 5e), which normally encompasses the area of higher SSTs anomalies during ENSO events.

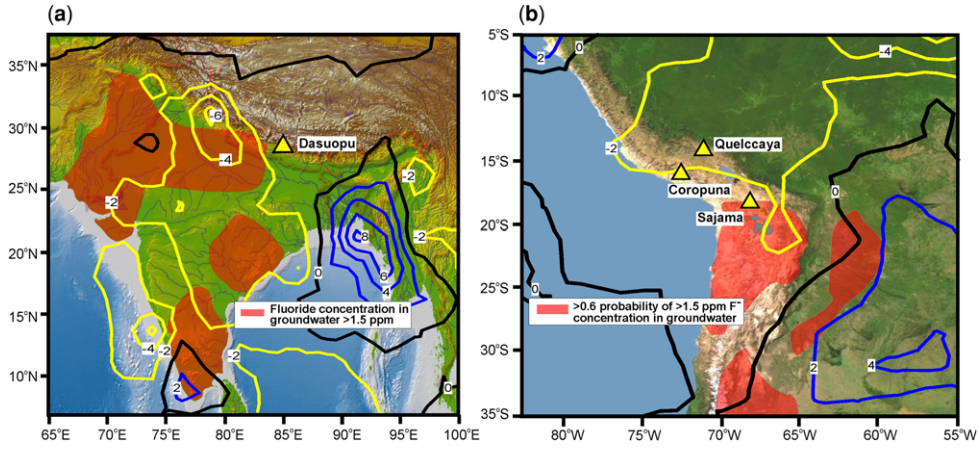

Fig. 6. Differences in average reanalysis wet season precipitation rates (mm/day) (Janowiak & Xie 1999) between El Niño and 'normal' years in (**a**) South Asia (June, July, August) and (**b**) eastern tropical South America (December, January, February). Yellow (negative)/blue (positive) contours indicate lower/higher precipitation rates during El Niño years. El Niño years are based on 3-month means of SST anomalies in the NIÑO3.4 region during the respective wet seasons (http://www.cpc.ncep.noaa.gov/products/analysis_monitoring/ensostuff/ensoyears.shtml). For South Asia the years with wet seasons in which the SST anomalies were above 0.5°C are: 1982, 1987, 1991, 1992, 1997, 2002, 2004, 2009 and 2015. For tropical eastern South America these years are: 1982/83, 1986/87, 1987/88, 1991/92, 1994/95, 1997/98, 2002/03, 2004/05, 2009/2010 and 2015/16. Precipitation rate data are from: http://iridl.ldeo.columbia.edu/SOURCES/.NOAA/.NCEP/.CPC/.CAMS_OPI/.v0208/.mean/.prcp/. Red shading indicates fluoride sources.

During an El Niño event there is a high probability for below-normal summer precipitation in many regions of monsoon India and southern Tibet (Fig. 6a). Under such conditions equatorial Pacific SSTs and the Walker circulation often reorganize and induce drought in South Asia. Normally, the variability of El Niño indicators such as SST indices and the Southern Oscillation Index (SOI) change directly with the all-India summer monsoon rainfall index (AISMRI) (Torrence & Webster 1999). However, the ENSO–ISM system is highly complex and variable such that drought in India is always associated with monsoon failure, but monsoon failure is not always associated with El Niño (Krishna Kumar *et al.* 2006). Their interaction has been characterized as a 'tangled' system (Webster *et al.* 1998) with no clear dominant component and with each component influencing the behaviour of the other. Their interdependence stems from the SST boundary conditions that are important for the development of both phenomena (Thompson *et al.* 2011). On longer timescales, the ENSO and ISM exhibit multi-decadal periods of high and low variance that reflect changes in oceanic and atmospheric processes. Periods of high/low variance in SSTs in El Niño index regions, SOI and the AISMRI occur with stronger/weaker relationships between ENSO and the ISM (Torrence & Webster 1999).

Across the Pacific Basin, the Altiplano of southern Peru and northern Bolivia also experiences below-normal wet season (DJF) precipitation during El Niño events (Fig. 6b). On the Altiplano, precipitation is governed by the position of the Bolivian High (BH), which develops from austral summer convection over the Amazon (Lenters & Cook 1997). During El Niño, decreased precipitation accompanies a weakening and/or northward movement of the BH.

The presence of an ENSO signal in the ice-core data is further tested using spectral analysis of the $\delta^{18}O$ and halogen concentration time series (Fig. 7a). The spectral analysis of the ice-core composites reveals significant periodicities amid the typical ENSO 3–7 year spectral band. Spectral analysis was performed for each ice-core record, but the stacked ice-core composites are used here for simplicity as they yielded similar results. The ice-core-derived F^- composite reveals multiple significant peaks in the 3–7 year band and the Cl^- composite exhibits spectral peaks similar to F^-; however, these peaks are just below 95% significance. For the $\delta^{18}O$ composite, a solitary significant peak occurs in the *c.* 3.67 year period. Although variations in the 3–7 year range are often attributed to ENSO, this link is only speculative. To verify the ENSO influence, coherence (or cross-spectra) analysis was also performed for the ice-core composites and the NIÑO3.4 index (Fig. 7b). The F^- composite exhibits two significant peaks in coherence with NIÑO3.4 at *c.* 6.3 and *c.* 3.3 years. The Cl^- composite shows significant coherence with NIÑO3.4 at *c.* 4 year

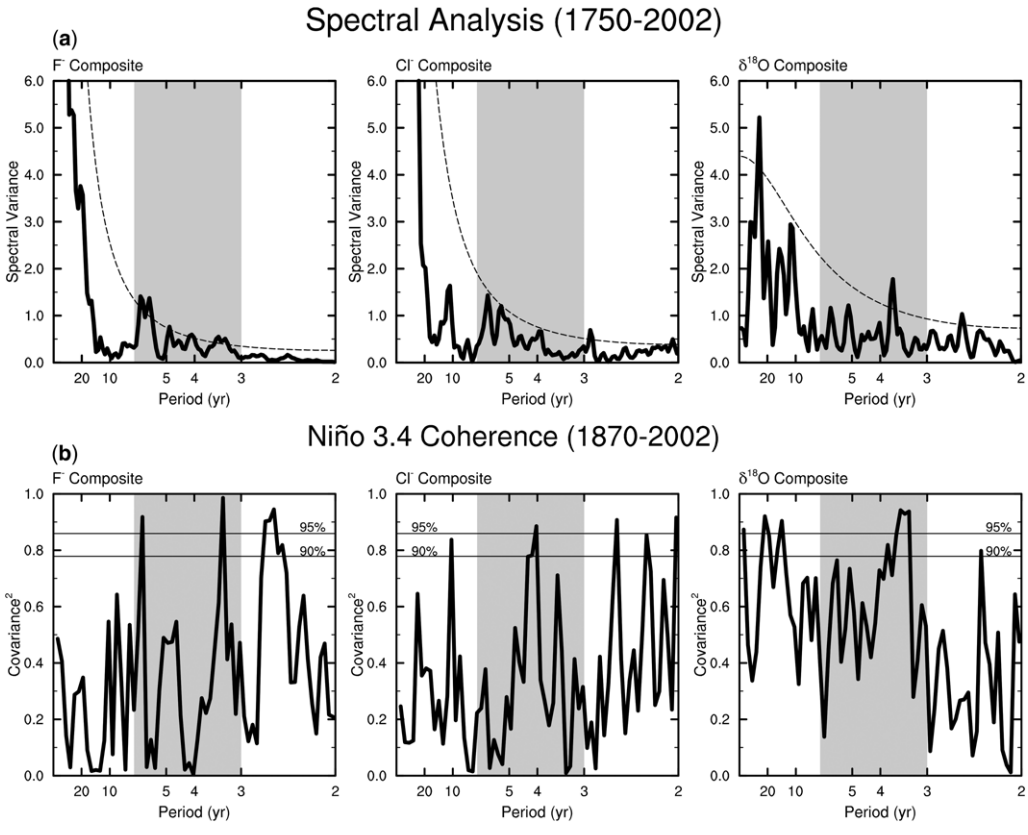

Fig. 7. (**a**) Spectral analysis of F^-, Cl^- and $\delta^{18}O$ ice-core composite (QSC, CCC, DSC) from 1750 to 2002 CE. Dashed line represents 95% confidence level for the Markov red noise spectrum. (**b**) Coherence analysis between the parameters in (a) and NIÑO3.4 SSTs from 1870 to 2002 CE. The 90% and 95% significance levels are marked. For these analyses, the mean was removed, the annual ice-core data were linearly detrended, and 10% tapering was applied as these are fairly common pre-treatment methods for data subjected to spectral analysis. A Daniell window of 3 was applied to smooth the sample spectra. The time periods used for the two analyses differ due to the lack of NIÑO3.4 data before 1870 CE. The typical ENSO 3–7 year spectral band is highlighted in grey.

periodicity, and the $\delta^{18}O$ composite shows coherence with NIÑO3.4 at *c.*3.4 years. The coherence analysis thereby validates that the significant cyclical patterns observed in the composite series are indeed associated with ENSO variability.

Intertropical convergence zone migration and major drought events over the last millennium

Because of the high resolution and more precise time control in the upper parts of the tropical ice-core records, most of the discussion so far has focused on the late-eighteenth-century dust peak. A similar aerosol peak is manifested by elevated concentrations of F^- and Cl^- in the mid-fourteenth century in the QSC (Fig. 3f) and also in the DSC by higher Cl^- and mineral dust concentrations (Fig. 8a, b). The earlier DSC event coincides with enriched $\delta^{18}O$ in speleothem (specifically stalagmite) records from east-central India (Fig. 8c) (Sinha *et al.* 2011) and NW China (Fig. 8d) (Zhang *et al.* 2008). The speleothem $\delta^{18}O$ values suggest drier conditions in the upwind dust source region which is dominated by the ISM and/or in a region dominated by the SE Asian monsoon (SEAM), or changes in the monsoon moisture source (Pausata *et al.* 2011; Mahar & Thompson 2012). Although the late-eighteenth century peak in the DSC is marked by very high concentrations of dust and most major ions (Table 1), the climatic conditions under which the aerosols were concentrated during these two periods were different. The more recent event occurred after a strengthening of the monsoons at *c.* 1700 CE (Sachs *et al.* 2009), although the Indian

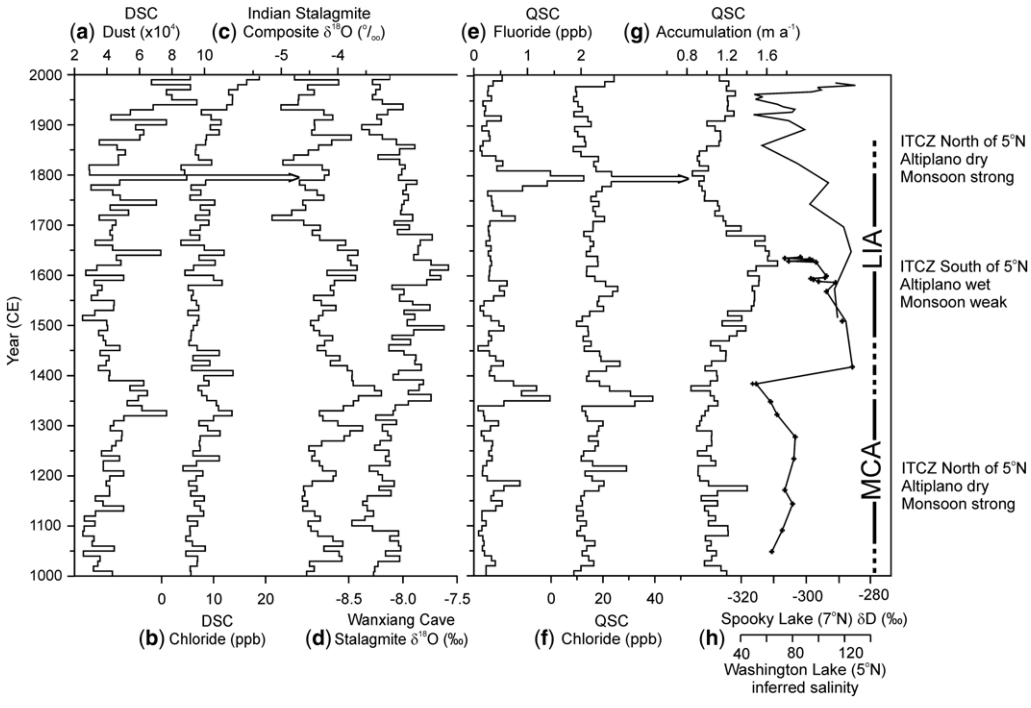

Fig. 8. Decadal averages over the last millennium for (**a**) DSC dust, (**b**) DSC Cl^-, (**c**) a composite speleothem record from east central India (Sinha *et al.* 2011), (**d**) a speleothem record from the Wanxiang Cave, NW China (Zhang *et al.* 2008), (**e**) QSC Fl^-, (**f**) QSC Cl^-, (**g**) QSC net accumulation and (**h**) equatorial lake chemistry records (Sachs *et al.* 2009). The Little Ice Age (LIA) and the Medieval Climate Anomaly (MCA) are marked; the dashed lines at either end denote dating ranges of the onset and termination.

speleothem record shows a brief isotopic enrichment (warmer, drier) from *c.* 1790 to *c.* 1820 CE as does the DSC $\delta^{18}O$ record (Thompson *et al.* 2000) (Table 1).

In contrast to the Dasuopu records, both the fourteenth- and eighteenth-century peaks in the QSC are characterized by high concentrations of F^- and Cl^- (Fig. 8e, f), but not by dust or other major ions (Table 1) (Thompson *et al.* 2013). They are concurrent with periods characterized by the lowest QSC net accumulation (A_n) values of the last millennium (Fig. 8g). During the twentieth century Quelccaya's net balance was broadly similar to Lake Titicaca levels (Thompson *et al.* 2013), and may therefore reflect large-scale precipitation changes over the Altiplano and the SW Amazon. In fact, proxy records of Lake Titicaca water levels show a minimum between *c.* 1050 and 1400 CE (Abbott *et al.* 1997), consistent with low accumulation in QSC over this period (Fig. 8g).

If the mid-fourteenth- and late-eighteenth-century aerosol events in the ice-core records are associated with the coupled ENSO-ISM system, then their uniqueness may arise from the spatially transitory nature of ENSO (Cook *et al.* 2010). This presents two questions: (1) are both events linked to ENSO; and (2) why are they so prominent in the ice cores when other major El Niño-associated droughts and monsoon failures are not? The ice-core records provide some evidence for linkages with El Niño conditions in the tropical Pacific Ocean. The $\delta^{18}O$ time series from all four cores contain enriched values during the late-eighteenth-century aerosol peaks (Table 1). As $\delta^{18}O$ in CCC, DSC and QSC are generally linked with SSTs in the equatorial Pacific (Figs 5d, e & 7), the enriched isotopic values associated with the two large aerosol events likely indicate warm phases of the ENSO cycle. However, as the ENSO/ISM linkage can weaken on interdecadal timescales (Torrence & Webster 1999), another process in addition to ENSO must be involved.

Threshold behaviour in the climate system, with its abundant amplifiers, can produce large changes with minimal forcing (Alley *et al.* 2003). Climate conditions which resulted in the late-eighteenth-century aerosol event in all four ice cores and the mid-fourteenth-century event in the QSC may have been influenced by the migration of the Intertropical Convergence Zone (ITCZ) from the end of the Medieval Climate Anomaly (MCA) in the fourteenth

century through the Little Ice Age (LIA), as recorded in the Cariaco Basin off the coast of Venezuela (Haug *et al.* 2001) and in island lakes in the equatorial Pacific Ocean (Fig. 8h) (Sachs *et al.* 2009). The Indian and Chinese speleothem records (Fig. 8c, d) and the QSC A_n record (Fig. 8g) show almost oppositely trending century-scale variations over the last millennium. The sudden influx of aerosols to the Himalayan and Andean glaciers may have occurred as the climate system crossed thresholds as conditions on the Altiplano and in south Asia changed with the migrating ITCZ. In the latter half of the fourteenth century, the ITCZ was positioned north of 5° N when the monsoons were more active as shown by depleted $\delta^{18}O$ speleothem values (Fig. 8c, d), and QSC A_n was low indicating dry conditions on the Altiplano (Fig. 8g). In the early 1400s CE the ITCZ moved southwards and remained close to the Equator for *c.* 300 years as the Altiplano became wetter and the monsoons weakened. Around 1700 CE, as the ITCZ moved back towards the north, the monsoons strengthened while Altiplano precipitation decreased (low QSC A_n), reaching its lowest level in the late-eighteenth to early-nineteenth centuries concomitant with the sudden increases in anion concentrations in the QSC (Fig. 8e, f) and the CCC (Fig. 3b). The late-eighteenth-century dust event in the DSC occurs with a short-term enrichment (warmer, drier conditions) in the Indian speleothem record (Fig. 8c) and the end of a brief southwards movement of the ITCZ (Fig. 8h). This might reflect a decade-long period of ENSO activity that occurred as the LIA was ending. This abrupt dry period is also observed in a total inorganic carbon profile from an East Java lake (Rodysill *et al.* 2013); however, the Java record contains no evidence of aridity in the fourteenth century. This may reflect a more northerly position of the southern extent of the ITCZ in the eighteenth century which did not occur earlier, although the Sachs *et al.* (2009) reconstruction in Figure 8h does not appear to support that interpretation. Another possibility involves a reduction in the eastwards shift of the intensified equatorial convection that characterizes warm episodes (Deser & Wallace 1990).

The mid-fourteenth-century event occurred just prior to the onset of the LIA (Fig. 8a, b) as the ITCZ moved southwards (Fig. 8h). QSC $\delta^{18}O$ values during the mid-fourteenth century are slightly elevated above background, suggesting slightly higher SSTs in the eastern and central tropical Pacific (Thompson *et al.* 2013). This has been noticed among many monsoon and ENSO proxy records during the mid-fourteenth to fifteenth centuries (Cook *et al.* 2010; Sinha *et al.* 2011), during which northwards shifts in the position of the monsoon trough may have produced drought in central India. In contrast, a record from Lake Pallcacocha (Ecuador) reveals that an increase in El Niño frequency occurred from *c.* 1350 to *c.* 1390 CE (Moy *et al.* 2002) while more negative coral $\delta^{18}O$ from Palmyra Island (6° N, 162° W) (Cobb *et al.* 2003) during this period could indicate drier conditions.

Abrupt climate events and black swans

Numerous studies have inferred that abrupt climate changes, including those caused by ENSO, have been important factors in epidemics, pandemics, famines and accompanying societal disruptions (McMichael 2012). The late-eighteenth-century aerosol peak which appears in tropical ice-core records is concurrent with the 'East India Drought', which has the 1791 CE El Niño at its core. Characterized by some as a 'mega-Niño' (Grove 2007), its effects were experienced throughout the monsoon regions in Asia and especially India, where it resulted in severe famine leading to *c.* 11 million deaths, with *c.* 600 000 alone in 1792 CE in the northern Circars of the Madras Presidency according to East India Company records. Historical and geological records show that other regions in the Eastern Hemisphere, such as Egypt and Australia (Grove & Chappell 2000) and Indonesia (Rodysill *et al.* 2013), experienced dramatic drought at this time. The consequences of the El Niños of the 1790s CE are also documented to a lesser extent in the Western Hemisphere, with flooding on the normally dry Peruvian coast that affected fishing and agriculture (Grove 2007), drought in NE Brazil and Mexico that caused crop failures, and arid conditions that extended to the Caribbean and islands in the southern tropical Atlantic (Grove & Chappell 2000).

Fewer historical records exist from the fourteenth century, particularly in South America, so linkages between El Niño-induced large-scale climate change and societal disruptions are more difficult to establish. In southern Peru, archaeological evidence indicates that unusual ENSO-linked flooding in coastal Peru *c.* 1350 CE may have been associated with the demise of the Chiribaya Culture (Satterlee 1993). Sufficient historical records from Europe and Asia exist that detail several significant fourteenth-century disasters, including the 'Black Death' which swept through much of the 'known' world. Roughly 30–60% of affected populations in Asia, India and Europe died from the plague that is believed to have begun in Central Asia, perhaps the Gobi Desert, during the Mongol Yuan Dynasty in the mid-fourteenth century, and was spread by nomadic Mongol horsemen. Unstable climate conditions in China and the Central Asian steppes, including alternating floods and droughts, are hypothesized to have resulted in migration of both human and infected rodent populations (McMichael 2012).

This climatic instability is recorded in the Wanxiang Cave speleothem record (Zhang *et al.* 2008), which shows above-average precipitation from summer monsoons until the early 1330s CE, followed by drought conditions until the end of the fourteenth century (Fig. 8d). European social and political structures underwent massive reorganization as population decimation ended the cheap, plentiful labour that supported the feudal system. Meanwhile, the unstable fourteenth-century climate may have exacerbated political upheaval in Medieval China. In 1368 CE, in the middle of an extreme drought from *c.* 1353 to *c.* 1395 CE (Zhang *et al.* 2008), the Chinese Ming Dynasty overthrew the Mongol Yuan Dynasty. The latter was founded by Khublai Khan in 1271 CE during an unusually warm and wet period in Mongolia which began at *c.* 1211 CE (Pederson *et al.* 2014). For most Chinese, 1368 CE is a key historical moment when the indigenous rebel regime expelled the Mongols and re-established their empire (Brook 2010).

The fate of glacier archives

The glaciers and ice caps of the Peruvian Andes and the Tibetan Plateau, like the majority of the tropical and mid-latitude, high-altitude cryosphere, are experiencing rapid and accelerating retreat as atmospheric temperatures rise (Bradley *et al.* 2006; Pepin & Lundquist 2008; You *et al.* 2008; Qin *et al.* 2009). The retreat of the Quelccaya ice cap is well documented (Thompson *et al.* 2006, 2013; Hanshaw & Bookhagen 2014), and the upper sections of the ice cap are experiencing melting and water percolation through the firn which is obliterating the climate record. Radiocarbon dating of plants collected near the margin of Quelccaya, which were exposed during recent ice retreat, suggests that this ice cap is the smallest it has been in the last 6000 years (Thompson *et al.* 2013). Other tropical ice fields are in imminent danger of disappearing by the middle of the twenty-first century, most notably Kilimanjaro in eastern Africa (Thompson *et al.* 2002, 2009) and the glaciers near Puncak Jaya in Papua, Indonesia (Thompson *et al.* 2011).

As of early 2017 almost one billion people live in the great Asian river basins, including the Ganges, Indus, Brahmaputra and Yangtze. These rivers are of vital importance to regional agriculture, power and aquifers, especially in regions that are less affected by summer monsoons, as they are the sources of meltwater. Across the Third Pole the most extensive glacier shrinkage is occurring in the Himalaya, characterized by the greatest reduction in glacier length, area and mass balance (Bolch *et al.* 2012; Yao *et al.* 2012). In the western Himalaya, the ice-core climate record from the Naimona'nyi glacier (NG in Fig. 1) indicates that the ice deposited since the mid-twentieth century has disappeared (Kehrwald *et al.* 2008). Although ice loss is an increasing concern in the Himalaya, in areas of the Hindu Kush and the western Pamirs the rate of glacier retreat is generally decreasing due to increasing precipitation (Bolch *et al.* 2012). Nevertheless, the global acceleration of ice loss has drastic implications for water resources in some of the most populous areas of the world, and is also contributing to global sea-level rise.

Climate changes projected over the twenty-first century and beyond include greater extremes in, and modified spatial patterns of, temperature and precipitation which will likely disrupt water supplies and agricultural productivity (Stocker *et al.* 2013). While uncertainty remains over how El Niño will change in a warmer world, recent studies suggest the potential for increasing frequencies of extreme events (Cai *et al.* 2014) and for the associated hydroclimate variability in sensitive regions such as southern Asia (Johnson 2014). Moreover, the life cycles and transmission of infectious agents affecting human, agriculture and animal systems is inextricably tied to climate and its variability (Altizer *et al.* 2013). Today, abrupt large-scale climate events such as those of the mid-fourteenth and late-eighteenth centuries would undoubtedly exacerbate the anticipated impacts of climate warming and result in greater food insecurity, water scarcity, changes in disease transmission, enhanced regional conflicts and population displacement. Recognition that the Earth system has experienced such events in the past under natural but unexpected circumstances, and will undoubtedly experience them in the future with the added complication of anthropogenic contributions, should prompt rapid action to increase the resilience of both human and natural systems upon which all Earth's inhabitants critically depend.

Directions for future research

The reconstruction of decadal- to centennial-scale tropical Pacific Ocean climate variability requires an array of low-latitude proxy records such as alpine ice cores from both the eastern and western sides of the ocean basin. Records from the southern slopes of the Himalaya are particularly valuable as they can provide information on the glaciological, meteorological and climatological processes in a region that is directly impacted by the Indian monsoon and by ENSO. Some of the highest and coldest low-latitude glaciers are located in Kashmir and in the Himachal Pradesh provinces in the far northwestern reaches of the southern slopes of the Himalaya. Efforts should therefore be made to extract long, high-resolution palaeoclimate records from glaciers

in this region. Such an undertaking, both in core retrieval and analysis, must be conducted in a collaborative international framework.

Funding was provided by NSF Awards ATM-0318430, ATM-0823586 and AGS-0443988, and The Ohio State University's Climate, Water and Carbon Program. We thank all the field and laboratory team members, many from BPCRC, who have worked over the years to acquire these ice cores and extract their preserved climate histories. We acknowledge the efforts of our Peruvian colleagues from the Servicio National de Meteorologia e Hidrologia, also C. Portocarrero, and our mountaineers led by B. Vicencio. We thank T. Yao and all our colleagues at the Institute of Tibetan Plateau Research and Cold and Arid Regions Environmental and Engineering Research Institute, Chinese Academy of Sciences without whose long-term collaboration the Dasuopu program could not have been accomplished. U. Schotterer at the University of Bern, Climate and Environment Physics Group conducted the tritium measurements on the Coropuna core. This is Byrd Polar and Climate Research Center Contribution Number 1565.

References

Abbott, M.A., Binford, M.W., Brenner, M. & Kelts, K.R. 1997. A 3500 ^{14}C yr high-resolution record of water-level changes in Lake Titicaca, Bolivia/Peru. *Quaternary Research*, **47**, 169–180, https://doi.org/10.1006/qres.1997.1881

Alley, R.B., Marotzke, J. *et al.* 2003. Abrupt climate change. *Science*, **299**, 2005–2010, https://doi.org/10.1126/science.1081056

Altizer, S., Ostfeld, R., Johnson, P.T.J., Kutz, S. & Harvell, C.D. 2013. Climate change and infectious diseases: from evidence to a predictive framework. *Science*, **341**, 514–519, https://doi.org/10.1126/science.1239401

Amini, M., Mueller, K. *et al.* 2008. Statistical modeling of global geogenic fluoride contamination in groundwaters. *Environmental Science & Technology*, **42**, 3662–3668.

Bolch, T., Kulkarni, A. *et al.* 2012. The state and fate of Himalayan glaciers. *Science*, **336**, 310–314, https://doi.org/10.1126/science.1215828

Bradley, R.S., Vuille, M., Hardy, D. & Thompson, L.G. 2003. Low latitude ice cores record Pacific sea surface temperatures. *Geophysical Research Letters*, **30**, 1174, https://doi.org/10.1029/2002GL016546

Bradley, R.S., Vuille, M., Diaz, H.F. & Vergara, W. 2006. Threats to water supplies in the Tropical Andes. *Science*, **312**, 1755–1756, https://doi.org/10.1126/science.1128087

Brook, T. 2010. *The Troubled Empire: China in the Yuan and Ming Dynasties*. MA thesis, Harvard University.

Cai, W., Borlace, S. *et al.* 2014. Increasing frequency of extreme El Niño events due to greenhouse warming. *Nature Climate Change*, **4**, 111–116, https://doi.org/10.1038/nclimate2100

Cobb, K.M., Charles, C.D., Cheng, H. & Edwards, R.L. 2003. El Niño/Southern Oscillation and tropical Pacific climate during the last millennium. *Nature*, **424**, 271–276, https://doi.org/10.1038/nature01779

Cook, E.R., Anchukaitis, K.J., Buckley, B.M., D'Arrigo, R.D., Jacoby, G.C. & Wright, W.E. 2010. Asian Monsoon failure and megadrought during the last millennium. *Science*, **328**, 486–489, https://doi.org/10.1126/science.1185188

Dalai, T.K., Krishnaswami, S. & Sarin, M.M. 2002. Major ion chemistry in the headwaters of the Yamuna river system: chemical weathering, its temperature dependence and CO_2 consumption in the Himalaya. *Geochimica et Cosmochimica Acta*, **66**, 3397–3416.

Deser, C. & Wallace, J.M. 1990. Large-scale atmospheric circulation features of warm and cold episodes in the tropical Pacific. *Journal of Climate*, **3**, 1254–1281, https://doi.org/10.1175/1520-0442(1990)003<1254:LSACFO>2.0.CO;2

Edmunds, W.M. & Smedley, P.L. 2013. Fluoride in natural waters. *In*: Selinus, O., Alloway, B., Centeno, J.A., Finkelman, R.B., Fuge, R., Lindh, U. & Smedley, P.L. (eds) *Essentials of Medical Geology*. Springer, New York, 311–336.

Grove, R.H. 2007. The great El Niño of 1789–93 and its global consequences: reconstructing an extreme climate event in world environmental history. *Medieval History Journal*, **10**, 75–98, https://doi.org/10.1177/097194580701000203

Grove, R.H. & Chappell, J. 2000. El Niño chronology and the history of global crises during the Little Ice Age. *In*: Grove, R.H. & Chappell, J. (eds) *El Niño – History and Crisis*. The White Horse Press, Cambridge, 5–34.

Hanshaw, M.N. & Bookhagen, B. 2014. Glacial areas, lake areas, and snow lines from 1975 to 2012: status of the Cordillera Vilcanota, including the Quelccaya Ice Cap, northern central Andes, Peru. *The Cryosphere*, **8**, 359–376, https://doi.org/10.5194/tc-8-359-2014

Haug, G.H., Hughen, K.A., Sigman, D.M., Peterson, L.C. & Röhl, U. 2001. Southward migration of the Intertropical Convergence Zone through the Holocene. *Science*, **293**, 1304–1308, https://doi.org/10.1126/science.1059725

Hren, M.T., Chamberlain, C.P., Hilley, G.E., Blisniuk, P.M. & Bookhagen, B. 2007. Major ion chemistry of the Yarlung Tsangpo-Brahmaputra river: chemical weathering, erosion, and CO_2 consumption in the southern Tibetan plateau and eastern syntaxis of the Himalaya. *Geochimica et Cosmochimica Acta*, **71**, 2907–2935, https://doi.org/10.1016/j.gca.2007.03.021

Huang, B., Banzon, V.F. *et al.* 2015. Extended reconstructed sea surface temperature version 4 (ERSST.v4). Part I: upgrades and intercomparisons. *Journal of Climate*, **28**, 911–930, https://doi.org/10.1175/JCLI-D-14-00006.1

Jacks, G., Bhattacharya, P., Chaudhary, V. & Singh, K.P. 2005. Controls on the genesis of some high-fluoride groundwaters in India. *Applied Geochemistry*, **20**, 221–228, https://doi.org/10.1016/j.apgeochem.2004.07.002

Janowiak, J.E. & Xie, P. 1999. CAMS_OPI: a global satellite-rain gauge merged product for real-time precipitation monitoring applications. *Journal of Climate*, **12**, 3335–3342, https://doi.org/10.1175/1520-0442(1999)012<3335:COAGSR>2.0.CO;2

Johnson, N.C. 2014. Atmospheric science: a boost in big El Niño. *Nature Climate Change*, **4**, 90–91, https://doi.org/10.1038/nclimate2108

KALNAY, E., KANAMITSU, M. *ET AL.* 1996. The NCEP/NCAR 40-year reanalysis project. *Bulletin of the American Meteorological Society*, **77**, 437–471, https://doi.org/10.1175/1520-0477(1996)077<0437:TNYRP>2.0.CO;2

KEHRWALD, N.M., THOMPSON, L.G. *ET AL.* 2008. Mass loss on Himalayan glacier endangers water resources. *Geophysical Research Letters*, **35**, L22503, https://doi.org/10.1029/2008GL035556

KRISHNA KUMAR, K., RAJAGOPALAN, B., HOERLING, M., BATES, G. & CANE, M. 2006. Unraveling the mystery of Indian Monsoon failure during El Niño. *Science*, **314**, 115–119, https://doi.org/10.1126/science.1131152

LENTERS, J.D. & COOK, K.H. 1997. On the origin of the Bolivian High and related circulation features of the South American climate. *Journal of the Atmospheric Sciences*, **54**, 656–678, https://doi.org/10.1175/1520-0469(1997)054<0656:OTOOTB>2.0.CO;2

LIU, W., HUANG, B. *ET AL.* 2015. Extended reconstructed sea surface temperature version 4 (ERSST.v4): Part II. Parametric and structural uncertainty estimations. *Journal of Climate*, **28**, 931–951, https://doi.org/10.1175/JCLI-D-14-00007.1

MAHAR, B.A. & THOMPSON, R. 2012. Oxygen isotopes from Chinese caves: records not of monsoon rainfall but circulation regime. *Journal of Quaternary Science*, **27**, 615–624, https://doi.org/10.1002/jqs.2553

MANN, M.E., CANE, M.A., ZEBIAK, S.E. & CLEMENT, A. 2005. Volcanic and solar forcing of the tropical Pacific over the past 1000 years. *Journal of Climate*, **18**, 447–456, https://doi.org/10.1175/JCLI-3276.1

MCMICHAEL, A.J. 2012. Insights from past millennia into climatic impacts on human health and survival. *Proceedings of the National Academy of Sciences*, **109**, 4730–4737, https://doi.org/10.1073/pnas.1120177109

MOY, C.M., SELTZER, G.O., RODBELL, D.T. & ANDERSON, D. M. 2002. Variability of El Niño/Southern Oscillation activity at millennial timescales during the Holocene epoch. *Nature*, **420**, 162–165, https://doi.org/10.1038/nature01194

PAUSATA, F.S.R., BATTISTI, D.S., NISANCIOGLU, K.H. & BITZ, C.M. 2011. Chinese stalagmite $\delta^{18}O$ controlled by changes in the Indian monsoon during a simulated Heinrich event. *Nature Geoscience*, **4**, 474–480, https://doi.org/10.1038/ngeo1169

PEDERSON, N., HESSL, A.E., BAATARBILEG, N., ANCHUKAITIS, K.J. & DI COSMO, N. 2014. Pluvials, droughts, the Mongol Empire, and modern Mongolia. *Proceedings of the National Academy of Sciences*, **111**, 4375–4379, https://doi.org/10.1073/pnas.1318677111

PEPIN, N.C. & LUNDQUIST, J.D. 2008. Temperature trends at high elevations: patterns across the globe. *Geophysical Research Letters*, **35**, L14701, https://doi.org/10.1029/2008GL034026

QIN, J., YANG, K., LIANG, S. & GUO, X. 2009. The altitudinal dependence of recent rapid warming over the Tibetan Plateau. *Climatic Change*, **97**, 321–327, https://doi.org/10.1007/s10584-009-9733-9

RAO, N.S. & DEVADAS, D.J. 2003. Fluoride incidence in groundwater in an area of Peninsular India. *Environmental Geology*, **45**, 243–251, https://doi.org/10.1007/s00254-003-0873-3

RAYNER, N.A., PARKER, D.E. *ET AL.* 2003. Global analyses of sea surface temperature, sea ice, and night marine air temperature since the late nineteenth century. *Journal of Geophysical Research*, **108**, **4407**, https://doi.org/10.1029/2002JD002670

RETTIG, S.L., JONES, B.F. & RISACHER, F. 1980. Geochemical evolution of brines in the Salar of Uyuni, Bolivia. *Chemical Geology*, **30**, 57–79, https://doi.org/10.1016/0009-2541(80)90116-3

ROCHE, M.A., BOURGES, J., CORTES, J. & MATTOS, R. 1992. Climatology and hydrology of the Lake Titicaca basin. *In*: DEJOUX, C. & ILTIS, A. (eds) *Lake Titicaca, a Synthesis of Limnological Knowledge*. Kluwer, Norwell MA, 63–83.

RODYSILL, J.R., RUSSELL, J.M., CRAUSBAY, S.D., BIJAKSANA, S., VUILLE, M., EDWARDS, R.L. & CHENG, H. 2013. A severe drought during the last millennium in East Java, Indonesia. *Quaternary Science Reviews*, **80**, 102–111, https://doi.org/10.1016/j.quascirev.2013.09.005

SACHS, J.P., SACHSE, D., SMITTENBERG, R.H., ZHANG, Z., BATTISTI, D.S. & GOLUBIC, S. 2009. Southward movement of the Pacific intertropical convergence zone AD 1400–1850. *Nature Geoscience*, **2**, 519–525, https://doi.org/10.1038/ngeo554

SATSANGI, G.R., LAKHANI, A., KHARE, P., SINGH, S.P., KUMARI, K.M. & SRIVASTAVA, S.S. 1998. Composition of rain water at a semi-arid rural site in India. *Atmospheric Environment*, **32**, 3783–3793, https://doi.org/10.1016/S1352-2310(98)00115-0

SATTERLEE, D.R. 1993. *Impact of a fourteenth century El Niño flood on an indigenous population near Ilo, Peru*. PhD thesis, University of Florida.

SAXENA, A., KULSHRESTHA, U.C., KUMAR, N., KUMARI, K.M. & SRIVASTAVA, S.S. 1996. Characterization of precipitation at Agra. *Atmospheric Environment*, **30**, 3405–3412, https://doi.org/10.1016/1352-2310(96)00049-0

SINHA, A., BERKELHAMMER, M., STOTT, L., MUDELSEE, M., CHANG, H. & BISWAS, J. 2011. The leading mode of Indian Summer Monsoon precipitation variability during the last millennium. *Geophysical Research Letters*, **38**, L15703, https://doi.org/10.1029/2011GL047713

STOCKER, T.F., QIN, D. *ET AL.* (eds) 2013. Climate Change 2013: The Physical Science Basis. *Contribution of Working Group I to the Fifth Assessment Report of the Intergovernmental Panel on Climate Change*. Cambridge University Press, Cambridge.

THOMPSON, L.G., MOSLEY-THOMPSON, E. & THOMPSON, P.A. 1992. Reconstructing interannual climate variability from tropical and subtropical ice core records. *In*: DIAZ, H. & MARKGRAF, V. (eds) *El Niño, Historical and Paleoclimatic Aspects of the Southern Oscillation*. Cambridge University Press, New York, 295–322.

THOMPSON, L.G., YAO, T. *ET AL.* 1997. Tropical climate instability: the last glacial cycle from a Qinghai-Tibetan ice core. *Science*, **276**, 1821–1825, https://doi.org/10.1126/science.276.5320.1821

THOMPSON, L.G., DAVIS, M.E. *ET AL.* 1998. A 25,000 year tropical climate history from Bolivian ice cores. *Science*, **282**, 1858–1864, https://doi.org/10.1126/science.282.5395.1858

THOMPSON, L.G., YAO, T., MOSLEY-THOMPSON, E., DAVIS, M. E., HENDERSON, K.A. & LIN, P.-N. 2000. A high-resolution millennial record of the South Asian Monsoon from Himalayan ice cores. *Science*, **289**, 1916–1919, https://doi.org/10.1126/science.289.5486.1916

Thompson, L.G., Mosley-Thompson, E. *et al.* 2002. Kilimanjaro ice core records: evidence of Holocene climate change in tropical Africa. *Science*, **298**, 589–593, https://doi.org/10.1126/science.1073198

Thompson, L.G., Davis, M.E., Mosley-Thompson, E., Lin, P.-N., Henderson, K.A. & Mashiotta, T.A. 2005. Tropical ice core records: evidence for asynchronous glaciation on Milankovitch timescales. *Journal of Quaternary Science*, **20**, 723–733, https://doi.org/10.1002/jqs.972

Thompson, L.G., Mosley-Thompson, E. *et al.* 2006. Abrupt tropical climate change: past and present. *Proceedings of the National Academy of Sciences*, **103**, 10536–10543, https://doi.org/10.1073/pnas.0603900103

Thompson, L.G., Brecher, H.H., Mosley-Thompson, E., Hardy, D.R. & Mark, B.G. 2009. Glacier loss on Kilimanjaro continues unabated. *Proceedings of the National Academy of Sciences*, **106**, 19770–19775, https://doi.org/10.1073/pnas.0906029106

Thompson, L.G., Mosley-Thompson, E., Davis, M.E. & Brecher, H.H. 2011. Tropical glaciers, recorders and indicators of climate change, are disappearing globally. *Annals of Glaciology*, **52**, 23–34.

Thompson, L.G., Mosley-Thompson, E., Davis, M.E., Zagorodnov, V.S., Howat, I.M., Mikhalenko, V.N. & Lin, P.-N. 2013. Annually resolved ice core records of tropical climate variability over the past *c.* 1800 years. *Science*, **340**, 945–950, https://doi.org/10.1126/science.1234210

Torrence, C. & Webster, P.J. 1999. Interdecadal changes in the ENSO-Monsoon system. *Journal of Climate*, **12**, 2679–2690, https://doi.org/10.1175/1520-0442(1999)012<2679:ICITEM>2.0.CO;2

Trenberth, K.E. & Hoar, T.J. 1997. El Niño and climate change. *Geophysical Research Letters*, **24**, 3057–3060, https://doi.org/10.1029/97GL03092

Walker, G. & Bliss, E.W. 1932. World Weather. *Memoirs of the Royal Meteorological Society*, **4**, 53–84.

Webster, P.J., Magaña, V.O., Palmer, T.N., Shukla, J., Tomas, R.A., Yanai, M. & Yasunari, T. 1998. Monsoons: processes, predictability, and the prospects for prediction. *Journal of Geophysical Research*, **103**, 14451–14510, https://doi.org/10.1029/97JC02719

Yao, T., Thompson, L.G. *et al.* 2012. Different glacier status with atmospheric circulations in Tibetan Plateau and surroundings. *Nature Climate Change*, **2**, 663–667, https://doi.org/10.1038/nclimate1580

You, Q., Kang, S., Pepin, N. & Yan, Y. 2008. Relationship between trends in temperature extremes and elevation in the eastern and central Tibetan Plateau, 1961–2005. *Geophysical Research Letters*, **35**, L04704, https://doi.org/10.1029/2007GL032669

Zhang, P., Cheng, H. *et al.* 2008. A test of climate, sun, and culture relationships from an 1810-year Chinese cave record. *Science*, **322**, 940–942, https://doi.org/10.1126/science.1163965